Freshwater impacts recorded in tetraunsaturated alkenones and alkenone sea surface temperatures from the Okhotsk Sea across millennial-scale cycles

Naomi Harada,[1] Miyako Sato,[1] and Tatsuhiko Sakamoto[2]

Received 28 December 2006; revised 26 February 2008; accepted 31 March 2008; published 2 July 2008.

[1] We present records of phytoplankton-produced alkenones down a long piston core, which reveal changes of sea surface temperature (SST) and sea surface salinity (SSS) in the southwestern Okhotsk Sea over the past 120 ka. Between 20 and 60 ka B.P., alkenone-derived temperatures typically increased by 6°C–8°C from periods corresponding, within a few hundred years, to stadials to those corresponding to interstadials recorded in Greenland ice cores. The abundance of $C_{37:4}$ alkenone relative to total C_{37} alkenones (percent $C_{37:4}$), a possible proxy for salinity, indicated that during most low SSS was associated with high SST. The warm freshwater events might be related to (1) a decline in the supply of saline water entering the Okhotsk Sea through the Soya Strait; (2) strengthening of the freshwater supply from the Amur River and precipitation over the Okhotsk Sea, associated mainly with increased Asian summer monsoon activity; and (3) the effect of melting sea ice. These findings increase our understanding of the close linkage between high and low latitudes in relation to climate change and the synchronicity of climate changes within a few centuries between the Pacific and the Atlantic sides of the Northern Hemisphere.

Citation: Harada, N., M. Sato, and T. Sakamoto (2008), Freshwater impacts recorded in tetraunsaturated alkenones and alkenone sea surface temperatures from the Okhotsk Sea across millennial-scale cycles, *Paleoceanography*, *23*, PA3201, doi:10.1029/2006PA001410.

1. Introduction

[2] Modern thermohaline circulation is considered to be controlled predominantly by the western boundary current in deep water [*Stommel and Arons*, 1960]. Recently, however, sea surface salinity (SSS) in the northern North Atlantic and the Southern Ocean has also been an important driving force of global thermohaline circulation [*Seidov and Haupt*, 2003]. However, SSS influences not only global circulation but also regional or basin-scale ventilation. At certain times during glacial events, SSS in the North Pacific may have predominantly controlled ocean circulation via increased North Pacific Intermediate Water (NPIW) formation [*Ohkushi et al.*, 2003].

[3] The Okhotsk Sea is a marginal sea that lies between 45°N and 60°N and between 135°E and 165°E in the northwestern Pacific (Figure 1). At present, two thirds of its surface is covered seasonally by sea ice. This sea ice plays a primary role in the formation of dense shelf water (DSW) [*Martin et al.*, 1998], the major source of ventilation (renewal) of Okhotsk Sea Intermediate Water (OSIW), which is an important contributor to NPIW [*Talley and Nagata*, 1995]. The formation rate of NPIW is controlled by the relationship between sea surface temperature (SST) and SSS in the source area.

[4] Autumn SST and SSS variations in the Okhotsk Sea are closely related to sea ice formation during the subsequent winter. High freshwater discharge from the Amur River during summer (annual mean discharge during 1970–2003: 7000–14000 $m^3\ s^{-1}$), in conjunction with a warm air mass over the Amur River basin (45°N–55°N, 110°E–135°E, defined by *Ogi and Tachibana* [2006]) and the Okhotsk Sea, causes autumn SSTs in the Okhotsk Sea to be warm, thus suppressing sea ice formation during the following winter (present winter sea ice coverage: $85–155 \times 10^4\ km^2$) [*Ogi and Tachibana*, 2006]. The suppression of sea ice formation causes a decrease in DSW formation, leading to a decline in the production rate of NPIW [*Itoh et al.*, 2003]. The extent and duration of sea ice coverage is also sensitive to global warming and cooling; the production rate of sea ice in the Okhotsk Sea is predicted to decrease greatly in the future as a result of global warming [*Aota*, 1999; *Itoh*, 2007]. Therefore, environmental change in the Okhotsk Sea is both a sensitive mirror reflecting global climate change and a driving force of regional climate change.

[5] Investigations of past environmental change in the Okhotsk Sea have shown that SST and sea ice coverage change abruptly on a millennial timescale [*Gorbarenko et al.*, 2004]. The abundance of $C_{37:4}$ alkenone relative to total C_{37} alkenones (percent $C_{37:4}$) that is related with salinity [*Rosell-Melé et al.*, 2002] has been measured in a sediment core from the central Okhotsk Sea [*Seki et al.*, 2005]. Higher values (20–35%) of percent $C_{37:4}$ were found during the last glacial period than during the Holocene, suggesting that SSS decreased during the last glacial period mainly as a

[1] Institute of Observational Research for Global Change, Japan Agency for Marine-Earth Science and Technology, Yokosuka, Japan.
[2] Institute for Research on Earth Evolution, Japan Agency for Marine-Earth Science and Technology, Yokosuka, Japan.

0883-8305/08/2006PA001410

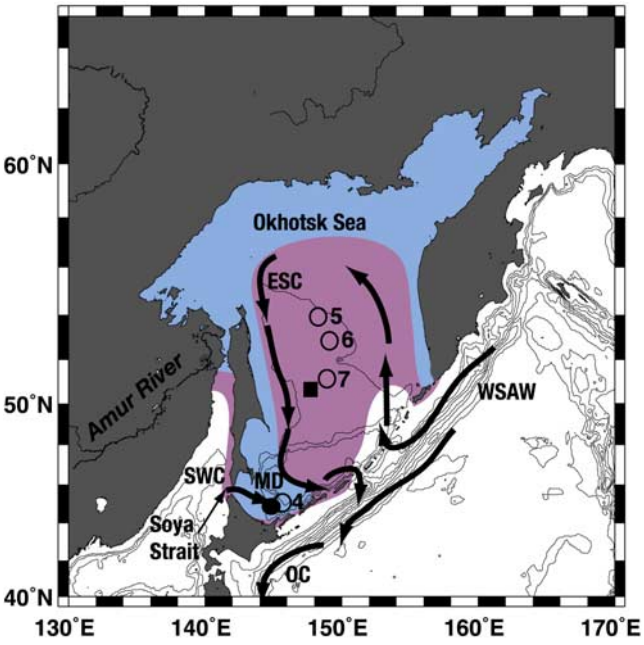

Figure 1. Map showing the sediment coring site, MD01-2412 (MD), in the southwestern Okhotsk Sea (solid circle, latitude 44°31′N, longitude 145°00′E, water depth, 1225 m). The four open circles are locations (station 4, latitude 44°31′N, longitude 144°59′E, water depth, 1161 m; station 5, latitude 54°19′N, longitude 149°16′E, water depth, 781 m; station 6, latitude 53°17′N, longitude 150°04′E, water depth, 1100 m; and station 7, latitude 51°16′N, longitude 149°12′E, water depth, 1201 m) at which suspended particles were sampled during cruise MR06-04 of the R/V *MIRAI*. The solid square is the sediment coring site reported by *Seki et al.* [2005]. The main water masses in this area are the Western Subarctic Water (WSAW), the East Sakhalin Current (ESC), the Oyashio Current (OC), and the Soya Warm Current (SWC). The bathymetry contour interval is 500 m. The light blue area shows the minimum extent of sea ice (2006), and the light blue and purple areas show its maximum extent (2001) during winters from 1996 to 2005 (see http://www.eorc.jaxa.jp/).

result of the expansion of seasonal sea ice and its melting. Ocean sea ice expansion events in the Okhotsk Sea during the past 100 ka were concurrent with high values of the Polar Circulation Index, an indicator of atmospheric circulation patterns in the Arctic that is strongly correlated with high-latitude ice sheet growth [*Mayewski et al.*, 1997], suggesting that such events are driven by active Arctic air circulation. The Arctic Oscillation (AO) is a dynamic atmospheric process by which pressure over the Arctic changes oppositely to that over midlatitudes in the Northern Hemisphere. The AO, with multidecadal cycles, influences air mass circulation over the Eurasian continent and its adjacent seas. Although we still have no direct records of past Arctic air circulation, reconstruction of the historical AO might provide new insight into the past climate system. In addition, although a substantial high-latitude, intra–Northern Hemisphere climate linkage between the Pacific and Atlantic sides has been recognized [*Seki et al.*, 2002], little is known about the mechanism of the climate linkage between high and low latitudes. Therefore, we used phytoplankton-produced alkenones to investigate millennial-scale changes in SST and SSS in the southwestern Okhotsk Sea over the past 120 ka and further clarify intra–Northern Hemisphere climate connections.

2. Samples and Methods

2.1. Sediments and Suspended Particles

[6] A 58.1-m-long sediment core (MD01-2412) was collected from the southwestern Okhotsk Sea by the *Marion Dufresne* as part of the International Marine Past Global Changes Study 2001 project (http://www.images-pages.org) (Figure 1). The core sediments consist of homogeneous diatom-bearing silty clay with volcanic ash layers and a major siliciclastic grain component. Changes in paleoproductivity in the MD01-2412 core on the basis of organic carbon content [*Ono et al.*, 2005], as well as changes in diatom and radiolarian assemblages [*Okazaki et al.*, 2005] and in the abundance of ice-rafted debris [*Sakamoto et al.*, 2006] have been reported.

[7] We constructed an age model by using multiple proxies: radiocarbon ages of planktonic foraminiferal tests (*Neogloboquadrina pachyderma*); oxygen isotopic stratigraphy of benthic foraminifera (*Uvigerina akitaensis* and *Uvigerina* spp.); and tephrochronology (Figure 2, modified from *Sakamoto et al.* [2006]). For sediments too old for ^{14}C chronology, we estimated their marine isotope stages (MISs) by comparing MD01-2412 data with typical peaks indicating glacial–interglacial intervals on the standard curve of $\delta^{18}O$ variation reported by *Martinson et al.* [1987]. By using this age model, we estimated sedimentation rates ranging from a minimum of 41.2 cm/ka during glacial periods to a maximum of 115.5 cm/ka during the Holocene. Samples were collected over the entire MIS 2–4 interval, and every 7.2 cm from other periods, for alkenone analysis. The time resolution of each sample (sample length, 2.4 cm) was estimated to average approximately 20 years in the Holocene, and 40 years in the glacial period.

[8] To be able to compare the exact timing of climate changes between the alkenone-derived temperature profiles and the $\delta^{18}O$ profile in Greenland ice cores (including the degree and direction of offset), absolute ages must be determined with high resolution. For example, the Bølling-Ållerød warm event (13–15 ka B.P.) and the Younger Dryas cold event (11.5–13 ka B.P.) occurred at about the same time on both the Atlantic and Pacific sides, with an age difference of only a few hundred years [*Nakagawa et al.*, 2003]. Because the MD01-2412 age model was constructed by using relative chronologies and a ^{14}C chronology (11 absolute ages) with an error of a few hundred years at least, its time resolution is insufficient to estimate the exact age difference of individual peaks and troughs between the alkenone-derived temperature profile and the $\delta^{18}O$ profile in the Greenland ice cores. Therefore, we considered the warm and cold events of the two profiles to have been simultaneous within a few hundred years.

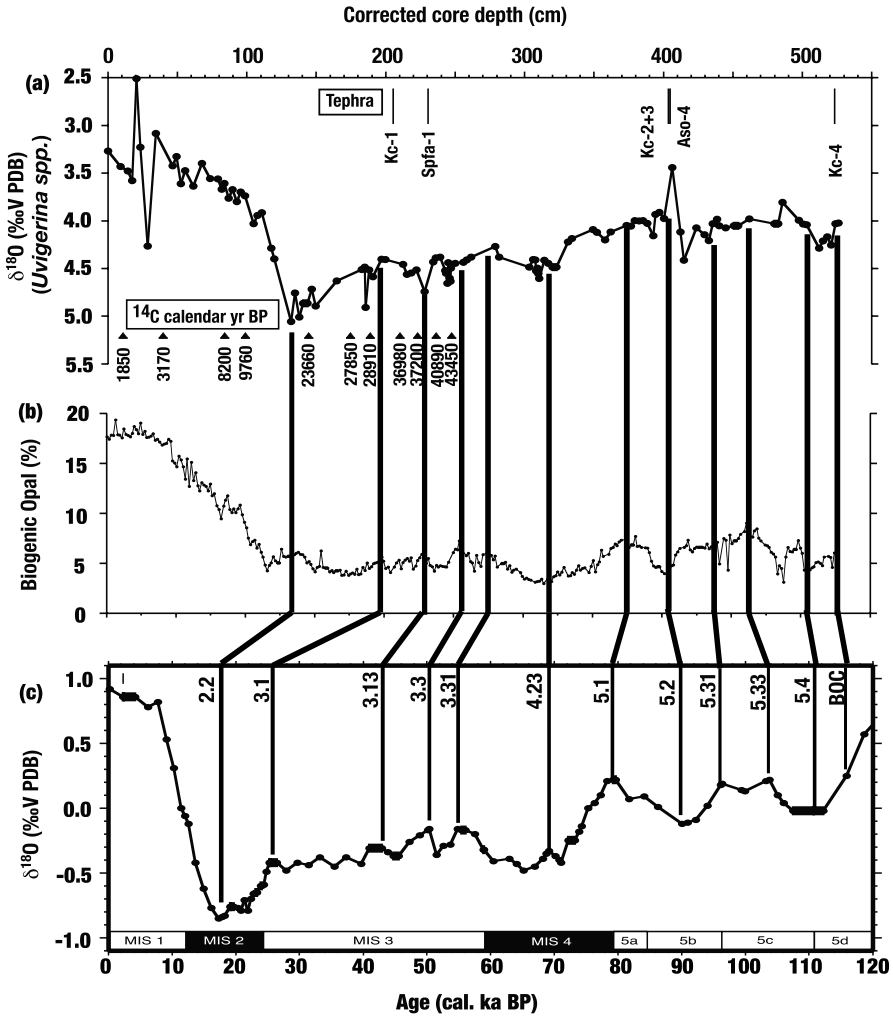

Figure 2. Multiple-proxy data for the age model of core MD01-2412. (a) The $\delta^{18}O$ stratigraphy of benthic foraminifera (*Uvigerina akitaensis* and *Uvigerina* spp.) (line connecting black dots). Radiocarbon ages of a planktonic foraminifer (*Neogloboquadrina pachyderma*) are shown as 11 small triangles labeled with ^{14}C calendar ages (year B.P.); tephra layers are Kc-1(Kuccharo-1, 30–35 ka); Spfa-1 (Shikotsu caldera, 40 ka); Kc-2 and Kc-3 (Kuttara caldera, 70 ka); Aso-4 (Aso caldera, 86–90 ka); and Kc-4 (100–130 ka). (b) Biogenic opal content and (c) stacked $\delta^{18}O$ curve [*Martinson et al.*, 1987] labeled with marine isotope stage (MIS) numbers. BOC is bottom of core. Modified from *Sakamoto et al.* [2006].

[9] To understand the relationship between alkenone-derived temperatures and modern in situ temperatures in the Okhotsk Sea, suspended particles were collected from the water column at four locations (stations 4, 5, 6, and 7) in the Okhotsk Sea, including one near the core site, during cruise MR06-04 of the R/V *MIRAI* (Figure 1). Seawater samples with a volume of 9–10 L were collected in Niskin bottles. The samples were filtered through GF/F filters (pretreated by heating to 450°C) on board to obtain the suspended particles.

2.2. Analytical Methods

[10] Bulk organic compounds were extracted from sediment core and suspended particle samples with an accelerated solvent extractor (ASE-200, DIONEX Japan Ltd., Osaka, Japan) at 100°C and 1500 psi (=10343 kPa) for 15 min. The solvent used was a mixture of distilled dichloromethane and methanol (99:1 v/v). The extracts were then saponified in 0.5 mol L^{-1} KOH in methanol at 80°C for 2 h. The neutral fraction was recovered with a pipette, dissolved in hexane, and then separated into subfractions by silica gel column chromatography using an automatic solid-preparation system (Rapid Trace SPE Workstation®, Zymark Center, Hopkinton, Massachusetts, United States). A ketone standard was used for the subfractionation (2-nonadecanone, Fluka Chemie, St. Gallen, Switzerland); the solvents used for each subfraction were the same as described previously [*Harada et al.*, 2003]. More than 90% of the 2-nonadecanone standard was recovered during this procedure. An aliquot of each alkenone fraction was gently concentrated under N_2 gas in an evaporator (Turbo Vap LV, Zymark Center), and then samples of each alkenone fraction

were analyzed by capillary gas chromatography using an Agilent 6890N gas chromatograph (Agilent Technologies, Inc., Santa Clara, California, United States) equipped with an HP-5MS fused-silica column (length, 60 m; inside diameter, 0.32 mm), a cold on-column injector, and a flame ionization detector. A hydrocarbon, dotriacontane, with deuterium (Cambridge Isotope Laboratories, Inc., Cambridge, Massachusetts, United States) and 2-nonadecanone were used as the internal standard and the yield standard, respectively. We assumed that the flame ionization detector was equally sensitive to C_{37} alkenone and the internal standard. Some of the alkenone samples were measured in duplicate, and the temperatures estimated from replicate analyses differed by less than 1°C.

2.3. Alkenone Temperature Calibration and Errors

[11] The alkenone unsaturation index, $U^{K'}_{37}$, which is the ratio of methyl alkenones with 37 carbon atoms and two double bonds to those with two or three double bonds [$U^{K'}_{37} = [C_{37:2}]/[C_{37:2} + C_{37:3}]$], is a proxy for surface water temperature [*Brassell et al.*, 1986; *Prahl and Wakeham*, 1987]. Several relationships between $U^{K'}_{37}$ and temperature have been proposed based on the core top and suspended particle calibrations [e.g., *Müller et al.*, 1998; *Conte et al.*, 2006]. In this study, we used the calibration equation $U^{K'}_{37} = 0.034T\ (°C) + 0.039$ [*Prahl et al.*, 1988].

[12] A major source of error in alkenone analyses is irreversible adsorption onto the chromatographic column [*Rosell-Melé et al.*, 2001; *Harada et al.*, 2006]. To reduce such error, it is necessary to inject a relatively large amount of alkenones into the gas chromatograph. We confirmed the relationships between the alkenone injection amount and the $U^{K'}_{37}$ value and between the injection amount and the calculated alkenone-derived temperature [*Harada et al.*, 2006]. When injection amounts were less than 12 ng, the calculated alkenone-derived temperatures were scattered within a range of 1.2°C; this scattering was slightly higher than the replication error of this study (<1°C). However, we judged that the alkenone data from those samples with low alkenone concentrations were sufficiently reliable for discussion of alkenone-derived temperatures. Because no samples in our data set had a concentration of less than 1 ng of alkenone per injection, all alkenone data, including those from samples with very low alkenone content, were used in this study.

[13] Some previous studies have reported that a small amount of another compound with a similar retention time to that of $C_{37:4}$ can influence the percent $C_{37:4}$ value [*Bendle et al.*, 2005; *Sicre et al.*, 2002], which is the amount of $C_{37:4}$ alkenone relative to the total amount of C_{37} alkenones and an alkenone-based proxy for SSS [e.g., *Rosell-Melé et al.*, 2002]. The common coeluting compound is probably derived from the plastic bags often used to store samples. However, we used glass bottles (pretreated by heating to 450°C) instead of plastic bags to store the sediment samples.

3. Results

3.1. Characteristics of Alkenone Particles in the Okhotsk Sea

[14] At present, the major alkenone producer in the Okhotsk Sea is *Emiliania huxleyi*, and alkenones are not known to be produced by this organism when the sea is covered by sea ice. Temperatures derived from alkenones in the suspended particles collected from the upper 100 m of the water column during 8–15 August 2006 were compared with the observed temperatures (Figure 3). A good correspondence between the alkenone-derived and observed temperatures was found in suspended-particle samples from 10 m water depth at station 4, the site at which the sediment core used in this study was collected, and at station 7. Interestingly, the data set shows that the alkenones were produced mainly in the upper 10 m of the water column, because alkenone-derived temperatures from suspended particles from below 10 m depth did not correspond to the observed in situ temperatures of the cold water mass known as the Okhotsk dichothermal water (DTW) [*Aota*, 1970] or the Okhotsk dichothermal layer (DTL) [*Yang and Honjo*, 1996]. This water mass is thought to be a remnant of winter convection and is found at 50–100 m depth from spring to autumn at this study site.

[15] On the other hand, at stations 5 and 6, alkenone-derived temperatures from suspended particle samples from 10 m water depth were lower than the observed temperatures. The sediment traps were deployed from August 1998 to June 2000 off Sakhalin (M4: 52°58′N, 145°29′E) [*Seki et al.*, 2007], where is close to our study sites of stations 5 and 6. The trap experiment indicated that alkenone-derived temperatures for August 1998 (no sample was available from August 1999) were about 5°C lower than the August satellite SST (advanced very high resolution radiometer, NOAA). Intra-annual alkenone-derived temperatures were almost the same as the observed September SST, but alkenone-derived temperatures showed a large difference between years (6°C–8°C in 1998 and 3°C–5°C in 1999) [*Seki et al.*, 2007]. Furthermore, the alkenone export in August 1998 was extremely low; alkenone production and exports occurred mainly during September and October. In addition, the total alkenone export in 1998 was almost six times that in 1999. The large interannual differences of alkenone production rate and alkenone-derived temperature and almost the same intra-annual alkenone-derived temperatures derived from the sediment trap experiment suggests that alkenone particles produced in September and October in both years remained in the water column during the following months. A relatively large contribution from such "old" suspended particles remaining in surface and subsurface waters could account for the large difference between the alkenone-derived and observed temperatures at stations 5 and 6, where alkenone-derived temperatures and alkenone concentrations at different depths varied over a broad range.

3.2. Mass Accumulation Rate of Alkenones in Core MD01-2412

[16] The mass accumulation rate (MAR) and content of C_{37} alkenones (percent) in the sediment were extremely low during 10–70 ka B.P. and 85–105 ka B.P., but, in contrast, were relatively high during 105–110 ka B.P., 70–85 ka B.P., and the Holocene (0–10 ka B.P.) (Figures 4a and 4b). This pattern is similar to that of the accumulation rate (AR) of total diatom valves in this sediment core (Figure 4d) [*Okazaki et al.*, 2005], although the increase in alkenone

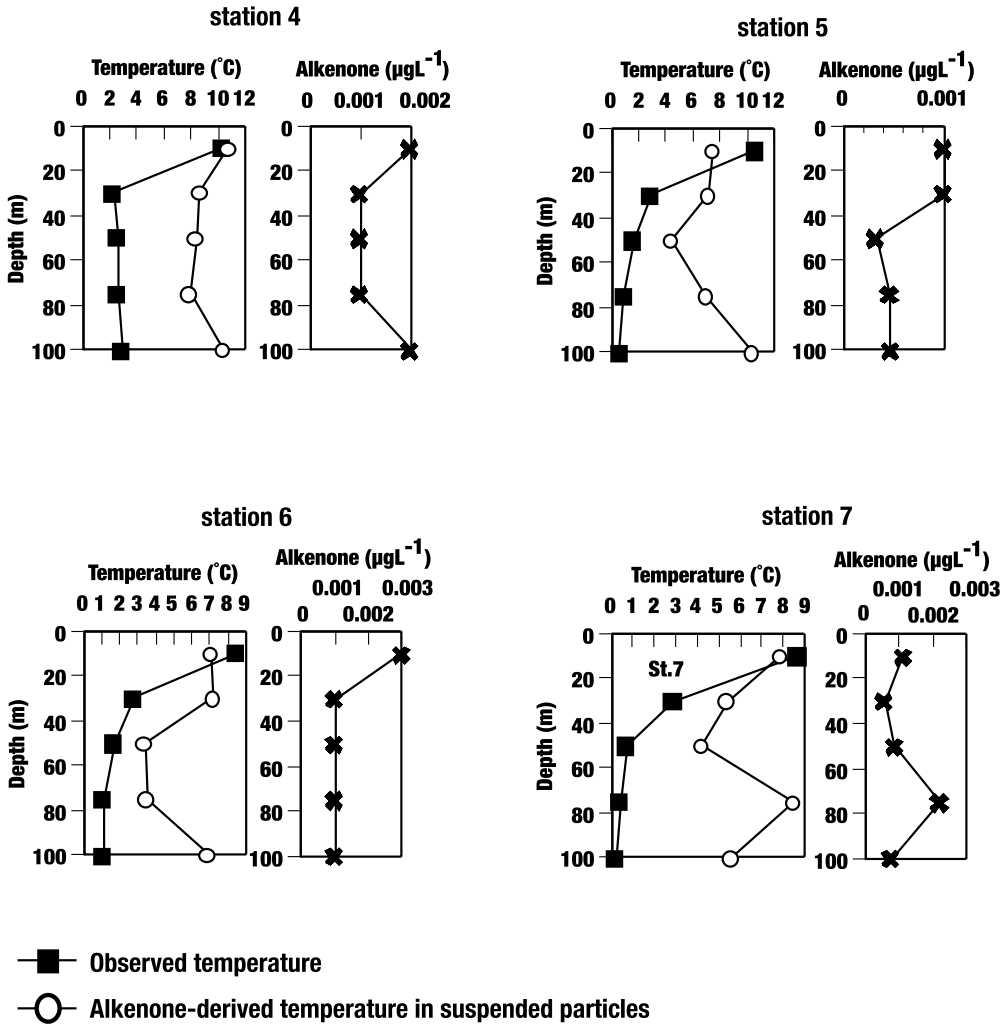

Figure 3. Alkenone-derived temperatures from suspended particles in water samples collected in the upper 100 m of the water column in the Okhotsk Sea, 8–15 August 2006 during cruise MR06-04 of the R/V *MIRAI*.

content slightly precedes that in diatoms during the Holocene. The ARs of valves of *Thalassiosira antarctica*, a diatom that lives in waters near sea ice, and of *Thalassiosira trifulta*, another cold-water diatom, were relatively high (Figures 4f and 4g) [*Okazaki et al.* [2005] during 25–60 ka B.P., when the alkenone MAR was very low. Moreover, the AR of *Thalassionema nitzschioides*, which is a warm-water diatom, was intermittently high during 30–60 ka B.P. (Figure 4e) [*Okazaki et al.*, 2005]. The variations of the ARs of these diatom species during periods of very low alkenone MARs suggest that during glacial periods sea ice coverage expanded seasonally and lasted longer, compared with during the modern period, but that warm-water episodes also occurred seasonally, during the short ice-free period in summer and autumn.

3.3. Alkenone-Derived SST at Core MD01-2412

[17] Alkenone-derived temperatures ranged from a minimum of 5°C at 41.9 ka B.P. to a maximum of 16.2°C at 25.9 ka B.P. and fluctuated abruptly between warm and cold events on a millennial timescale (Figure 5a) [*Harada et al.*, 2006]. Between 20 and 60 ka B.P., alkenone-derived temperatures typically increased by 6°C–8°C from the cold periods to warm periods (Figure 5a). These warm alkenone-derived temperatures recorded from the Okhotsk Sea are mostly concurrent with interstadials, with some notable exceptions such as stages 2 and 12, recorded in $\delta^{18}O$ values from the Greenland Ice Sheet Project 2 (GISP2) core (Figure 5c).

3.4. Alkenone-Derived SSS at Core MD01-2412

[18] We also considered SSS changes indicated by the alkenone-based proxy percent $C_{37:4}$. Although percent $C_{37:4}$ is still difficult to use as a conventional proxy for quantifying salinity globally [*Sikes and Sicre*, 2002], its levels are inversely correlated with regional salinity changes at high latitudes in both the Atlantic (Nordic Sea [*Bendle et al.*, 2005]; northeastern Atlantic [*Rosell-Melé et al.*, 2002];

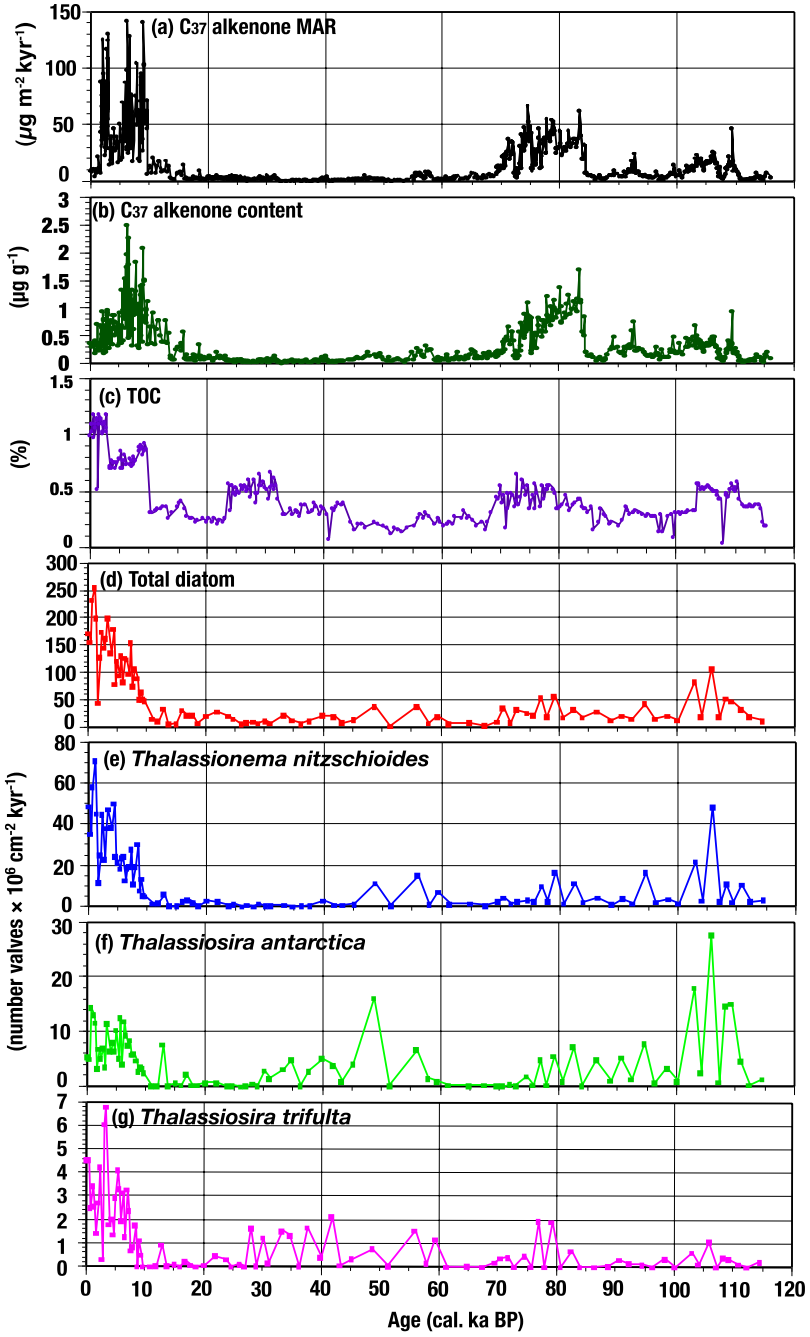

Figure 4. (a) Mass accumulation rate (MAR) of C_{37} alkenones ($C_{37:2}$ + $C_{37:3}$ + $C_{37:4}$) and (b) C_{37} alkenone content [*Harada et al.*, 2006] in MD01-2412, (c) total carbon content (TOC) [*Ono et al.*, 2005] and accumulation rates of diatom valves: (d) total diatoms; (e) *Thalassionema nitzschioides*; (f) *Thalassiosira Antarctica*, and (g) *Thalassiosira trifulta* [*Okazaki et al.*, 2005].

Baltic Sea [*Schulz et al.*, 2000]) and Pacific (Bering Sea [*Harada et al.*, 2003]) oceans, and in lakes at high latitude, such as Greenland Lake [*D'Andrea and Huang*, 2005], or high altitude, such as Lake Qinghai in China [*Liu et al.*, 2006]. Low salinity is thought to impose stress on the production mechanism of alkenones, thus accelerating $C_{37:4}$ production [*Harada et al.*, 2003; *Blanz et al.*, 2005].

[19] Another possible explanation for relatively high percent $C_{37:4}$ values is that they were produced by a different alkenone producer. The possibility of a species other than *E. huxleyi* being the alkenone producer can be evaluated by examining the production pattern of C_{38} alkenones. For example, although *E. huxleyi* synthesizes both C_{38} methyl and C_{38} ethyl alkenones, C_{38} alkenones in

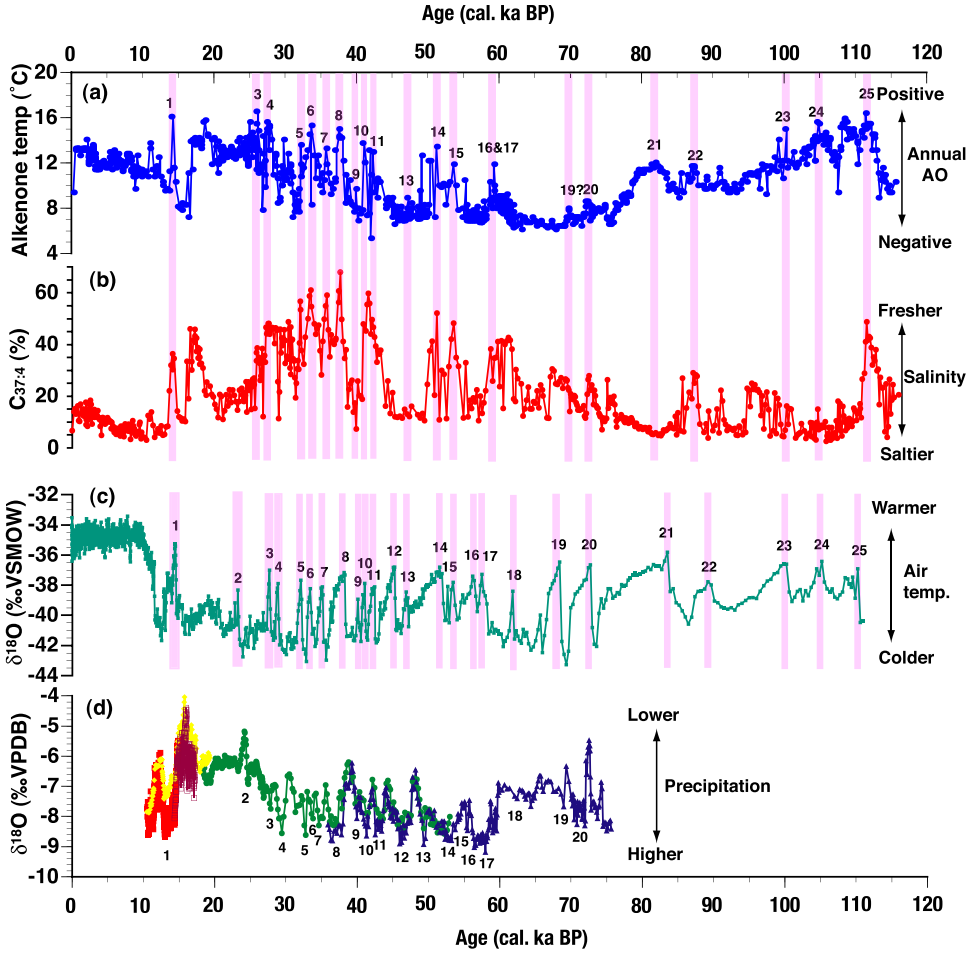

Figure 5. Alkenone-derived temperatures and content of $C_{37:4}$ alkenones relative to total C_{37} alkenone content (percent $C_{37:4}$) in the Okhotsk Sea, as recorded in MD01-2412, compared with other paleoclimatic data sets. (a) Alkenone-derived temperature and (b) percent $C_{37:4}$ in MD01-2412, (c) $\delta^{18}O$ variation recorded in the Greenland Ice Sheet Project 2 (GISP2) ice core, a proxy for air temperature (Vienna standard mean ocean water (VSMOW)) [*Grootes and Stuiver*, 1997], and (d) $\delta^{18}O$ variation recorded in stalagmites from Hulu Cave, a proxy for precipitation (Vienna Peedee belemnite standard (VPDB)) [*Wang et al.*, 2001]. Pink bars indicate interstadials, which are numbered in accordance with the GISP2 record. AO is Arctic Oscillation.

particle samples with relatively high percent $C_{37:4}$ values from the Baltic Sea are composed of only C_{38} ethyl alkenones [*Schulz et al.*, 2000; *Blanz et al.*, 2005], and neither $C_{38:2}$ methyl nor $C_{38:2}$ ethyl alkenones were detected in particles with extremely high percent $C_{37:4}$ values (77%) from the polar East Greenland Current. In surface waters of the Nordic Sea, although $C_{38:4}$ methyl and ethyl alkenones were detected in particles with $C_{37:4}$ alkenones, they were not detected in particles without $C_{37:4}$ alkenones [*Bendle et al.*, 2005]. We compared the chromatograms of C_{38} alkenones between the high alkenone-derived temperature sample from 111.3 ka B.P., which had a relatively high (41%) percent $C_{37:4}$ value, and the low alkenone-derived temperature sample from 71.5 ka B.P., with a relatively low (15%) percent $C_{37:4}$ value (Figure 6). In the chromatogram for 111.3 ka B.P. (Figure 6b), the relative abundances of the C_{38} ethyl alkenones (compounds 4, 6, and 8) were slightly higher than those of the C_{38} methyl alkenones (compounds 5, 7, and 9), as in previous studies [*Schulz et al.*, 2000; *Zink et al.*, 2001; *Blanz et al.*, 2005]. The chromatogram of a series of C_{38} alkenones from the sample for 71.5 ka B.P. (Figure 6a) was not drastically different from that for 111.3 ka B.P.; that is, a complete lack of C_{38} methyl alkenones was not found, although no $C_{38:4}$ ethyl alkenone was detected. On the other hand, for 111.3 ka B.P., the total abundance of a series of C_{38} alkenones (ΣC_{38} alkenones) was higher in contrast with that of a series of C_{37} alkenones (ΣC_{37} methyl alkenones) and the ratio of ΣC_{37} methyl alkenones to ΣC_{38} alkenones ($\Sigma C_{37}/\Sigma C_{38}$) was 0.56. For 71.5 ka B.P., the ΣC_{38} alkenones was close to that of ΣC_{37} methyl alkenones and the value of $\Sigma C_{37}/\Sigma C_{38}$ was 1.16. The $\Sigma C_{37}/\Sigma C_{38}$ of two samples from 71.5 ka B.P. and 111.3 ka B.P. are similar as that for *E. huxleyi* (0.91–2.26) and for *Gephyrocapsa oceanica (G. oceanica)* (0.59–0.81),

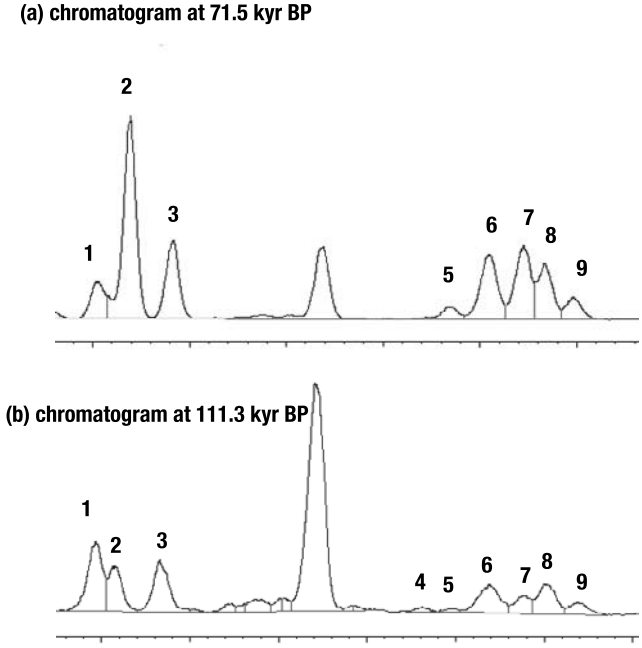

Figure 6. Portions of gas chromatograms of the alkenone fraction from samples showing (a) the stadial at 71.5 ka B.P. and (b) interstadial 25 at 111.3 ka B.P. Compounds identified by gas chromatograph–mass spectrometry are 1, $C_{37:4}$ methyl alkenone (Me); 2, $C_{37:3}$Me; 3, $C_{37:2}$Me; 4, $C_{38:4}$ ethyl alkenone (Et); 5, $C_{38:4}$Me; 6, $C_{38:3}$Et; 7, $C_{38:3}$Me; 8, $C_{38:2}$Et; and 9, $C_{38:2}$Me.

another alkenone producer, respectively [*Volkman et al.*, 1995]. This result, the $\Sigma C_{37}/\Sigma C_{38}$ of sample from 111.3 ka B.P. was within a range of $\Sigma C_{37}/\Sigma C_{38}$ for *G. oceanica*, suggests that *G. oceanica* may have also been possible alkenone contributor for 111.3 ka B.P.. Although *G. oceanica* is not major alkenone producer in present Okhotsk Sea, this species could possibly have been transported via the SWC from the Japan Sea to our study site. The *G.* oceanica, same strain existing in the Okhotsk Sea was collected from Tsugaru Strait and was cultured (K. Kimoto, unpublished data, 2008). We analyzed alkenone of this cultured strain and found that this strain did not produce $C_{37:4}$. Therefore, percent $C_{37:4}$ for *E. huxleyi* may be useful as a paleo-SSS indicator in present study, although unknown different producers would prevent the qualitative use of the percent $C_{37:4}$ as a proxy for salinity.

[20] In the sediments, percent $C_{37:4}$ varied between 3.31% and 68.7%, and its fluctuations corresponded to those in the alkenone-derived temperature record (Figure 5b). High percent $C_{37:4}$ values (fresher water) occurred concurrently with high alkenone-derived temperature, except during the period corresponding to interstadial 21. The glacial MAR of C_{37} alkenones was highest, second only to the Holocene MAR, during the period from 75 to 85 ka B.P. (Figure 4a). Both the period corresponding to interstadial 21 and the Holocene are characterized by warm, saline surface water in the Okhotsk Sea (Figures 5a and 5b). This high MAR suggests that suitable conditions for the growth of the alkenone producer were present for a longer part of the year during the period corresponding to interstadial 21, unlike during the other warm periods, implying that the alkenone producer can grow well in not only low-salinity waters but also in more saline waters. On the other hand, relatively low percent $C_{37:4}$ values (saltier water) were typically concurrent with low alkenone-derived temperatures during cold periods.

4. Discussion

4.1. Alkenone SSTs in Okhotsk and Its Adjacent Seas

[21] The alkenone-derived temperatures near the core top, 9°C–12°C, correspond to the monthly averaged temperature in August–September, the main alkenone production season at present at this study site [*Seki et al.*, 2007]. The correspondence of the alkenone-derived temperatures to the temperature during the major alkenone production season rather than to the annual average temperature is a common feature in the Okhotsk Sea [*Ternois et al.*, 2000; *Seki et al.*, 2004] and adjacent seas (Japan Sea [*Ishiwatari et al.*, 2001; *Fujine et al.*, 2006; *Lee*, 2007] and the subarctic gyre in the North Pacific [*Harada et al.*, 2004]).

[22] The lowest alkenone-derived temperature, 6.9°C, was obtained at 16.3 ka B.P., during the deglaciation; this temperature is lower than any temperatures associated with the last glacial maximum (LGM) (19–23 ka B.P.). A lower alkenone-derived temperature during the deglaciation than during the LGM has also been reported by previous studies in the Okhotsk Sea [*Ternois et al.*, 2000; *Seki et al.*, 2004] and the Japan Sea [*Ishiwatari et al.*, 2001; *Fujine et al.*, 2006; *Lee*, 2007], whereas in the North Pacific, the lowest alkenone-derived temperature occurred during the LGM [*Harada et al.*, 2004].

[23] Millennial-timescale increases in the alkenone-derived temperatures during periods corresponding to interstadial intervals at this study site (6°C–8°C) were high compared with the increase of about 4°C in alkenone-derived temperatures during interstadials reported from sites in the eastern North Pacific [*Seki et al.*, 2002]. One reason for the high alkenone-derived SSTs during interstadials might be that the alkenone producer species changed to one for which a different temperature calibration might be needed. An important component of the haptophyte flora from the Californian margin is *G. oceanica*. However, under natural conditions, alkenones from *G. oceanica* show a relationship with SST close to that of Prahl's temperature calibration equation [*Prahl et al.*, 1988] for *E. huxleyi* [*Herbert et al.*, 1998]. In addition, culture experiments using various *E. huxleyi* and *G. oceanica* strains have shown that the $U^{K'}_{37}$ versus SST relationship of *G. oceanica* falls within the range of the relationships calculated for cultured strains of *E. huxleyi* [*Conte et al.*, 1998]. Thus, even if the relative contributions of these two alkenone producers differed over geological time, the alkenone-derived SST estimated with Prahl's calibration equation should not deviate from reasonable values.

[24] Another reason for the high alkenone-derived temperatures might be advection of reworked alkenones from onshore sediment deposits in association with sea level

changes during the glacial period. The total organic carbon content (TOC) (Figure 4c) of MD01-2412 core frequently increased during the period corresponding to interstadials [*Ono et al.*, 2005]. In addition, the TOC to total nitrogen ratio (C/N molar ratio), which is an indicator of whether the organic materials originated predominantly from marine (a ratio of 4–10) or terrestrial (~20) sources, increased during the period corresponding to interstadials. We attribute these abrupt increases in the TOC and C/N ratio during the period corresponding to interstadials to an influx of sediments of terrigenous origin. However, the TOC and C/N ratio results also suggest that if there are reworked alkenones in the core sediments, their abundance is likely to be very small relative to that of the other terrigenous materials and therefore such reworked alkenones cannot account for the high alkenone SSTs during interstadials. Hence, we consider the high alkenone-derived SSTs corresponding to interstadials to be a feature of this study site and discuss possible causes below.

4.2. Salinity Anomalies and Their Cause

[25] The mechanism causing the high SST values in the Okhotsk Sea during interstadials can be understood in relation to the simultaneous SSS changes. High percent $C_{37:4}$ values, which we have inferred to be strongly related to low salinity, were found during most interstadials in association with high alkenone-derived temperatures (Figure 5b). It has been reported that anomalously high alkenone-derived temperatures detected in Japan Sea sediments during 15–20 ka B.P. might be related to low-salinity stress, although exactly what salinity range is meant by "low salinity" is not specified [*Fujine et al.*, 2006]. In the case of *E. huxleyi* in the Bering Sea, the $U^{K'}_{37}$ produced by the 2001 bloom corresponded to the in situ SST (with the calibration of *Prahl et al.* [1988]) at salinity values ranging from 30 to 32 [*Harada et al.*, 2003]. Because the salinity near MD01-2412 ranges from 32.5 to 33.2 (see http://pacificinfo.ru/en/), it is unlikely that significantly low salinity occurs at present at this study site. However, the $U^{K'}_{37}$ values might reflect physiological stress caused by low salinity (<30) during glacials, because a SSS of less than 30 was more likely during periods of lower sea level, when the relatively warm and saline Soya Warm Current (SWC) would not have flowed into the Okhotsk Sea. Therefore, we hypothesized the existence of three different types of freshwater impacts to explain these concurrent relatively freshwater and high-SST events.

[26] The first impact is a decline in the supply of saline water entering the Okhotsk Sea through the Soya Strait. At present, the SWC is the main source of warm (7–20°C) but saline (33.6–34.3) water to the southwestern Okhotsk Sea [*Takizawa*, 1982]. However, during the glacial period, the contribution of the SWC would have been small or absent because the shallow Soya Strait (55 m deep) through which the SWC enters the Okhotsk Sea would have been silled because of the low eustatic sea level [*Bard et al.*, 1990; *Chappell et al.*, 1996; *Rabineau et al.*, 2006].

[27] The second impact is the supply of freshwater from the Amur River and precipitation over the Okhotsk Sea. The East Sakhalin Current, which receives water from the Amur River, contributes a low-salinity water mass to the western Okhotsk Sea. At 55°N, 142°E, near the source of the East Sakhalin Current, the salinity is 32.5 in September, about 0.9 lower than during the rest of the year (see http://pacificinfo.ru/en/). The Amur discharge is highest during August–October (the season of east Asian summer monsoon precipitation and melting snow and frozen soil at high altitudes), and the summer–autumn discharge is remarkably warm (about 20°C [*Ogi et al.*, 2001, and references therein]). In addition, the presence of cold DTW (50–100 m) just beneath the warm low-salinity surface water would inhibit convection between the surface and subsurface water masses; consequently, shallow stratification at the surface would be stably maintained, and the surface water mass would be easily warmed during the summer–autumn. Therefore, the combination of a high summer–autumn Amur discharge, associated mainly with Asian summer monsoon precipitation, and cold DTW in the subsurface may have had a large effect on surface thermohaline conditions in the Okhotsk Sea over geological time.

[28] The third impact is the effect of melting sea ice. We have suggested that the period of sea ice coverage was longer during glacials than at present, perhaps lasting almost year-round, except in midsummer, and as a result probably shifting the season of alkenone production to the ice-free midsummer period. This hypothesis implies also that, because the ice melted only in midsummer, meltwater from the in situ sea ice could have further lowered the SSS. Moreover, the changed thermal budget of the surface water mass, a consequence of the increased stratification of the surface water caused by increased precipitation and melting sea ice, would also have contributed to high alkenone-derived temperatures.

[29] Is there any evidence to show that the supply of freshwater increased during interstadials, thereby accounting for the high SST and low SSS in the southwestern Okhotsk Sea during these warm intervals? The oxygen isotope record in stalagmites from Hulu Cave, near Nanjing, China, shows that changes in precipitation are controlled by Asian summer monsoon activity and that precipitation was strong during interstadials (Figure 5d) [*Wang et al.*, 2001]. Because the intensity of the Asian summer monsoon directly influences the summer–autumn Amur discharge, we propose that enhanced Asian summer monsoon precipitation during interstadials caused the warm river discharge to the Okhotsk Sea from the Amur to increase, resulting in abrupt warm-SST and low-SSS episodes during the last glacial period. An enhanced Asian summer monsoon would also have intensified the supply of warm, moist air masses over the Okhotsk Sea, further influencing the thermohaline conditions in the surface water. An increase in precipitation at 15 ka B.P., corresponding to the Bølling-Ållerød warm event, in Siberia [*Chebykin et al.*, 2002] also supports the validity of this "freshwater impact hypothesis."

4.3. Pacific-Atlantic Climate Connection

[30] According to *Ogi and Tachibana* [2006], the maximum sea ice coverage area over the Okhotsk Sea ($85–155 \times 10^4$ km^2) is negatively correlated with the annual mean Amur discharge (7000–14000 m^3 s^{-1}) on a decadal time-

scale, and both the summer discharge and the maximum winter sea ice area are strongly affected by the annual integrated AO. A positive annual AO pattern (negative anomalies near the pole and positive anomalies at Okhotsk Sea latitudes *Thompson and Wallace* [1998]) causes the anomalous horizontal convergence of moisture fluxes over the Amur River basin and the Okhotsk Sea, resulting in increased Amur discharge. Moreover, a positive annual AO pattern causes warmer atmospheric temperatures over the Okhotsk Sea, resulting in warm autumn SSTs [*Ogi and Tachibana*, 2006]. Although the AO effect is dominant during winter, the SST anomaly induced by the AO persists for several months. The winter AO index correlates well with east Asian summer precipitation on an interdecadal timescale, owing to planetary wave propagation from the North Atlantic to the North Pacific [*Sung et al.*, 2006].

[31] Our data show not only that the high-SST events associated with freshwater impacts were correlated with interstadials but also that low-SST events associated with saline water were correlated with stadials (Figures 5a and 5b). Autumn SSTs in the Okhotsk Sea, estimated as alkenone-derived temperatures in this study, might be related to the AO pattern during past periods. Any discussion of the AO during the glacial period must assume that AO-like conditions existed throughout the glacial period. *Justino and Peltier* [2005] simulated the North Atlantic Oscillation (NAO), another dynamic atmospheric process on the Atlantic side with a signal corresponding to that of the AO, during the LGM in a paleoclimate model. Despite the presence of glacial ice sheets, which would have strongly influenced glacial wintertime atmospheric circulation over the ocean, the NAO apparently existed during the glacial period [*Justino and Peltier*, 2005].

[32] Climatic differences across Dansgaard-Oeschger cycles are summarized in Figure 7. When the annual integrated AO pattern is positive, the pressure difference between the Arctic region and midlatitudes is large and polar jet circulation is strong, with the result that southward penetration of cold air masses from the Arctic region to midlatitudes is inhibited. Consequently, the air temperature at Okhotsk Sea latitudes is relatively warm. Then, warm, fresh water covers the surface of the Okhotsk Sea during summer–autumn, also perhaps as a result of the northward expansion of the east Asian summer monsoon area. When the annual integrated AO pattern is negative, the pressure difference between the Arctic region and midlatitudes is small and the polar jet is weak. As a result, cold air masses easily penetrate from the Arctic region to midlatitudes, and as a consequence the air temperature at Okhotsk Sea latitudes becomes colder. Thus, assuming that the AO existed during the glacial period, as simulated by paleoclimate modeling, high SSTs in the Okhotsk Sea during interstadials may be related to a positive annual integrated AO pattern, and low SSTs during stadials to a negative pattern. A teleconnection via the atmospheric dynamics over the Arctic region and midlatitudes of the Northern Hemisphere might thus explain the observed climatic connection between Greenland (North Atlantic side) and the Okhotsk Sea (North Pacific side). However, it is still questionable whether there was a relationship between the AO and east Asian summer monsoon activity during glacial periods. To understand the mechanism, origin, and propagation of quasi-abrupt climate changes, many more investigations based on insights obtained from both paleoproxies and modeling of changes in the balance between atmospheric and ocean impacts on multiple timescales are necessary.

[33] On the other hand, ocean circulation in association with atmospheric dynamics is another possible explanation for the teleconnection, within a few centuries, between the North Atlantic and North Pacific. A freshwater hosing simulation, carried out off Greenland and designed to evaluate the impact of freshwater supplied to the ocean during Pleistocene stadial periods, suggests that immediate cooling caused by weakened thermal transport due to less ventilation by the Atlantic meridional overturning circulation (AMOC) would have occurred as a result of an increase in freshwater, and that the tropical SST variations associated with a weakened AMOC would also have led to meridional changes in the Intertropical Convergence Zone (ITCZ) [*Timmermann et al.*, 2007]. As a result, the ITCZ would have shifted southward, with corresponding diabatic forcing changes, eventually generating a Rossby wave train in the atmosphere that would have resulted in an intensified Aleutian Low, thereby cooling the northern North Pacific. Although some of the models explain simultaneous cooling in the North Atlantic and the North Pacific by an intensified AO (negative AO) in winter, other results do not show any good relationship between AO intensification and cooling in the North Pacific (A. Timmermann, personal communication, 2007). Thus, more investigations are needed to understand the relationship between atmospheric dynamics, including the role of the AO signal, and Atlantic-Pacific climate teleconnections on millennial timescales.

[34] The presence of warm, fresh surface water would have inhibited active sea ice formation on the northern continental shelf in the Okhotsk Sea, resulting in a low production rate of DSW and consequently inhibiting the production of OSIW and NPIW. During stadials, relatively cold, saline water covered the surface of the Okhotsk Sea, owing to easier penetration of cold air masses from the Arctic region to Okhotsk Sea latitudes, which might have resulted in active sea ice formation, a high production rate of DSW, and, consequently, active production of OSIW and

Figure 7. Summary diagram of climate features during (a) interstadials and (b) stadials at this study site (black circle) and in the surrounding region. Monthly mean precipitation of more than 3 mm/d in the region from 30°S to 50°N and from 30°E to 150°W, averaged over 1979–1998 (from climate.gsfc.nasa.gov/iotw/20060908114104_med.jpg), is shown in pink (bottom left). Heavy rainfall in southeastern China, starting in May and ending in August, is associated with the Asian summer monsoon [e.g., *Chang*, 2004]. This rainfall regime is also associated with the Mei-yu front, a warm, wet air mass that extends from southeastern China to Japan and its vicinity during spring-summer.

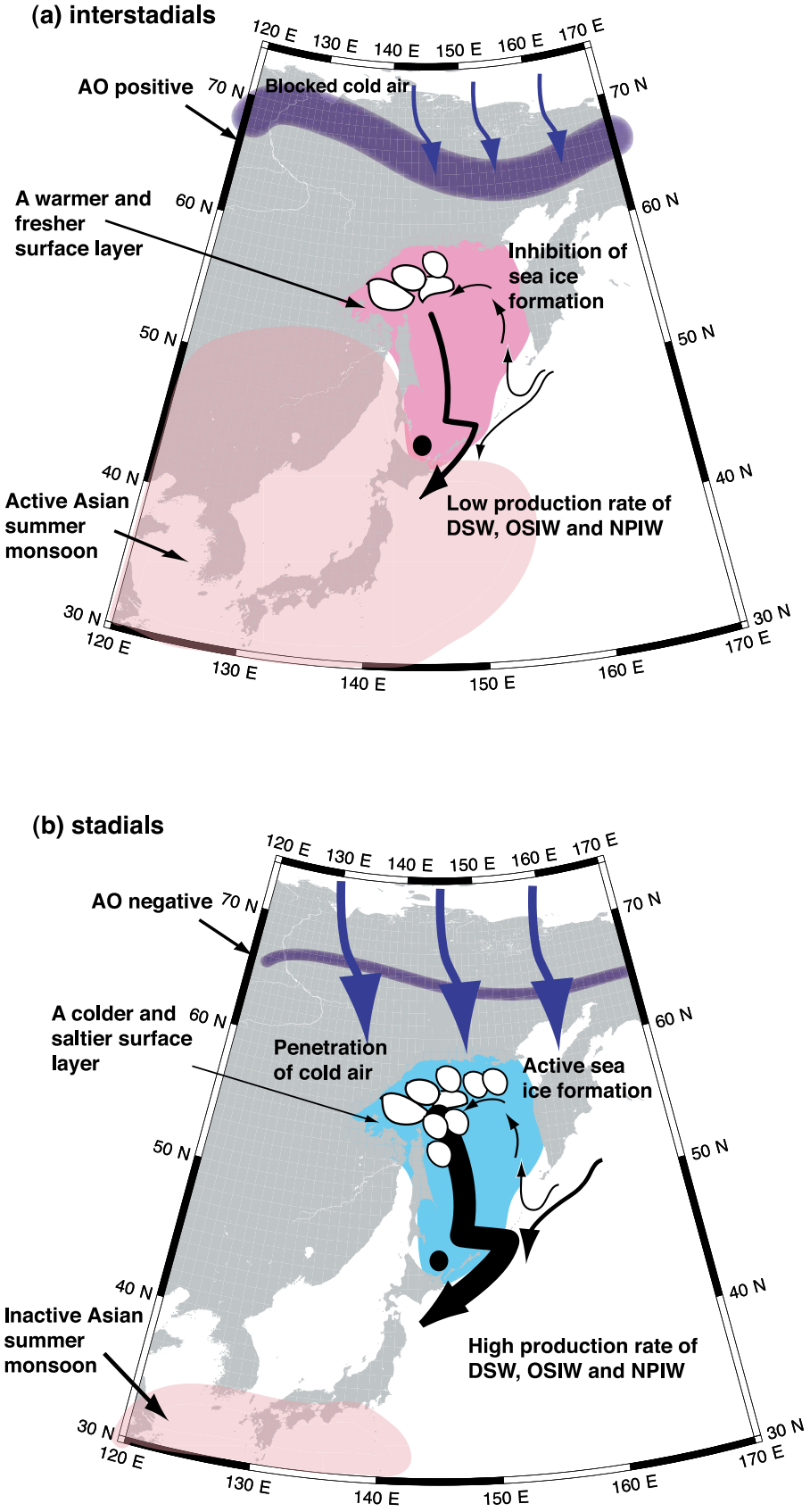
(a) interstadials
AO positive
Blocked cold air
A warmer and fresher surface layer
Inhibition of sea ice formation
Active Asian summer monsoon
Low production rate of DSW, OSIW and NPIW
(b) stadials
AO negative
A colder and saltier surface layer
Penetration of cold air
Active sea ice formation
Inactive Asian summer monsoon
High production rate of DSW, OSIW and NPIW
120 E
130 E
140 E
150 E
160 E
170 E
70 N
60 N
50 N
40 N
30 N

Figure 7

NPIW. *Ahagon et al.* [2003] reported that the ventilation at mid depth (1300 m) in the northwestern North Pacific declined during the Bølling-Ållerød warm event (13–15 ka B.P.) and strengthened during the Younger Dryas cold event (11.5–13 ka B.P.). These findings support the validity of our scenario.

5. Conclusion

[35] We obtained modern alkenone-derived temperatures by analyzing suspended particles and those for the past 120 ka by analyzing sediment core samples from the southwestern Okhotsk Sea. Our results and suggested explanations are summarized as follows:

[36] 1. Alkenone-derived temperatures from suspended particles collected at station 4, where the sediment core used in this study was collected, and station 7 showed that alkenones are produced mainly in the upper 10 m of the water column. At stations 5 and 6, however, alkenone-derived temperatures of suspended-particle samples from 10 m water depth were lower than the observed temperatures. The alkenone production season is very short, limited mostly to September, but the alkenone particles might remain in the water column during subsequent months [*Seki et al.*, 2007]. Such remaining particles might have caused the relatively large difference between the alkenone-derived and observed temperatures at stations 5 and 6.

[37] 2. The MAR and content of C_{37} alkenones (percent) in the sediments were extremely low during 10–70 ka B.P. and 85–105 ka B.P., but, in contrast, were relatively high during 105–110 ka B.P., 70–85 ka B.P., and the Holocene (0–10 ka B.P.). This pattern is similar to that of the AR of total diatom valves, although the increase in alkenone content slightly precedes that in diatoms during the Holocene. The combination of very low alkenone MARs and variations in the ARs of diatom species during glacial periods suggests that sea ice coverage expanded seasonally and lasted longer, compared with during the modern period, but that warm-water episodes also occurred occasionally, perhaps in summer and autumn.

[38] 3. Alkenone-derived temperatures of the sediment core ranged from 5°C to 16.2°C and abruptly fluctuated between warm and cold events on a millennial timescale. Between 20 and 60 ka B.P., alkenone-derived temperatures typically increased by 6–8°C between periods corresponding to the stadials and interstadials recorded in the Greenland ice cores. We used the alkenone-based proxy, percent $C_{37:4}$, to detect SSS changes and found that high percent $C_{37:4}$ values (fresher water) occurred simultaneously with high alkenone-derived temperature periods. Such high SSTs during interstadials could be related to physiological stress caused by low salinity. We hypothesize that these high-SST and low-SSS episodes in the Okhotsk Sea can be explained by the existence of three different types of freshwater impacts: (1) a decline in the supply of saline water entering the Okhotsk Sea through the Soya Strait; (2) strengthening of the freshwater supply from the Amur River and precipitation over the Okhotsk Sea, associated mainly with increased Asian summer monsoon activity; and (3) the effect of melting sea ice.

[39] Climate changes are synchronous, within a few centuries, between the Pacific and the Atlantic sides of the Northern Hemisphere, and atmospheric dynamics, possibly related to the AO pattern, and changes in the AMOC formation rate might explain this synchronicity. During Pleistocene stadial periods, abrupt cooling was likely caused by weakened thermal transport due to less ventilation by the AMOC, and tropical SST variations associated with a weakened AMOC also led to meridional changes in the ITCZ [*Timmermann et al.*, 2007]. As a result, the ITCZ shifted southward, generating a Rossby wave train in the atmosphere and resulting in an intensified Aleutian Low, thereby cooling the northern North Pacific.

[40] Our study demonstrates that sea surface conditions at Okhotsk Sea latitudes not only are regulated by the high-latitude intrahemispheric atmosphere–ocean circulation system but also are closely related to east Asian summer monsoon activity, which is controlled by atmosphere–ocean interaction at low latitudes.

[41] **Acknowledgments.** We are grateful to T. Nakatani for her help with the sample preparation and alkenone analysis in the laboratory. We thank H. Kawahata for organizing and providing financial support for the IMAGES coring cruise near Japan. We also thank the Editor, G. Dickens, and the Associate Editor, E. Sikes, of *Paleoceanography* and two reviewers, J. Bendle and Y. Huang, for giving us important comments for improving this manuscript. This work was supported by the Japan Agency for Marine-Earth Science and Technology. In addition, a part of this work was supported by a grant from the Japan Society for the Promotion of Science (JSPS Bilateral Joint Projects).

References

Ahagon, N., K. Ohkushi, M. Uchida, and T. Mishima (2003), Mid-depth circulation in the northwest Pacific during the last deglaciation: Evidence from foraminiferal radiocarbon ages, *Geophys. Res. Lett.*, *30*(21), 2097, doi:10.1029/2003GL018287.

Aota, M. (1970), Study of the variation of oceanographic condition north-east off Hokkaido in the Sea of Okhotsk II (in Japanese with English abstract), *Low Temp. Sci., Ser. A*, *28*, 261–279.

Aota, M. (1999), Long-term tendencies of sea ice concentration and air temperature in the Okhotsk Sea coast of Hokkaido, *PICES Sci. Rep. 12*, 1–2, Inst. of Ocean Sci., Sidney, B.C., Canada.

Bard, E., B. Hamelin, and R. G. Fairbanks (1990), U-Th ages obtained by mass spectrometry in corals from Barbados: Sea level during the past 130,000 years, *Nature*, *346*, 456–458, doi:10.1038/346456a0.

Bendle, J., A. Rosell-Melé, and P. Ziveri (2005), Interannual variability and paleoceanographic implications of unusual distributions of alkenones in the surface waters of the Nordic seas, *Paleoceanography*, *20*, PA2001, doi:10.1029/2004PA001025.

Blanz, T., K.-C. Emeis, and H. Siegel (2005), Controls on alkenone unsaturation ratios along the salinity gradient between the open ocean and the Baltic Sea, *Geochim. Cosmochim. Acta*, *69*, 3589–3600, doi:10.1016/j.gca.2005.02.026.

Brassell, S. C., G. Eglinton, I. T. Marlowe, U. Pflaumann, and M. Sarnthein (1986), Molecular stratigraphy: A new tool for climatic assessment, *Nature*, *320*, 129–133, doi:10.1038/320129a0.

Chang, C.-P. (Ed.) (2004), *East Asian Monsoon*, 564 pp., World Sci., Hackensack, N. J.

Chappell, J., A. Omura, T. Esat, M. McCulloch, J. Pandolfi, Y. Ota, and B. Pillans (1996), Reconciliation of late Quaternary sea levels derived from coral terraces at Huon Peninsula

with deep sea oxygen isotope records, *Earth Planet. Sci. Lett.*, *141*, 227–236, doi:10.1016/0012-821X(96)00062-3.

Chebykin, E. P., D. N. Edgington, M. A. Grachev, T. O. Zheleznyakova, S. S. Vorobyova, N. S. Kulikova, I. N. Azarova, O. M. Khlystov, and E. L. Goldberg (2002), Abrupt increase in precipitation and weathering of soils in east Siberia coincident with the end of the last glaciation (15 cal kyr BP), *Earth Planet. Sci. Lett.*, *200*, 167–175, doi:10.1016/S0012-821X(02)00588-5.

Conte, M. H., A. Thompson, D. Lesley, and R. P. Harris (1998), Genetic and physiological influences on the alkenone/alkenoate versus growth temperature relationship in *Emiliania huxleyi and Gephyrocapsa oceanica*, *Geochim. Cosmochim. Acta*, *62*, 51–68, doi:10.1016/S0016-7037(97)00327-X.

Conte, M. H., M.-A. Sicre, C. Rühlemann, J. C. Wever, S. Schulte, D. Schulz-Bull, and T. Blanz (2006), Global temperature calibration of the alkenone unsaturation index ($U^{K'}_{37}$) in surface waters and comparison with surface sediments, *Geochem. Geophys. Geosyst.*, *7*, Q02005, doi:10.1029/2005GC001054.

D'Andrea, W. J., and Y. Huang (2005), Long chain alkenones in Greenland lake sediments: Low δ^{13}C values and exceptional abundance, *Org. Geochem.*, *36*, 1234–1241, doi:10.1016/j.orggeochem.2005.05.001.

Fujine, K., M. Yamamoto, R. Tada, and Y. Kido (2006), A salinity-related occurrence of a novel alkenone and alkenoate in late Pleistocene sediments from the Japan Sea, *Org. Geochem.*, *37*, 1074–1084, doi:10.1016/j.orggeochem.2006.05.004.

Gorbarenko, S. A., J. R. Southon, L. D. Keigwin, M. V. Cherepanova, and I. G. Gvozdeva (2004), Late Pleistocene–Holocene oceanographic variability in the Okhotsk Sea: Geochemical, lithological and paleontological evidence, *Palaeogeogr. Palaeoclimatol. Palaeoecol.*, *209*, 281–301, doi:10.1016/j.palaeo.2004.02.013.

Grootes, P. M., and M. Stuiver (1997), Oxygen 18/16 variability in Greenland snow and ice with 10^{-3}- to 10^{5}-year time resolution, *J. Geophys. Res.*, *102*, 26,455–26,470, doi:10.1029/97JC00880.

Harada, N., K.-H. Shin, A. Murata, M. Uchida, and T. Nakatani (2003), Characteristics of alkenones synthesized by a bloom of *Emiliania huxleyi* in the Bering Sea, *Geochim. Cosmochim. Acta*, *67*, 1507–1519, doi:10.1016/S0016-7037(02)01318-2.

Harada, N., N. Ahagon, M. Uchida, and M. Murayama (2004), Northward and southward migrations of frontal zones during the past 40 kyr in the Kuroshio-Oyashio transition area, *Geochem. Geophys. Geosyst.*, *5*, Q09004, doi:10.1029/2004GC000740.

Harada, N., N. Ahagon, T. Sakamoto, M. Uchida, M. Ikehara, and Y. Shibata (2006), Rapid fluctuation of alkenone temperature in the southwestern Okhotsk Sea during the past 120 kyr, *Global Planet. Change*, *53*, 29–46, doi:10.1016/j.gloplacha.2006.01.010.

Herbert, T. D., J. D. Schuffert, D. Thomas, C. Lange, A. Weinheimer, A. Peleo-Alampay, and J. C. Herguera (1998), Depth and seasonality of alkenone production along the California margin inferred from a core top transect, *Paleoceanography*, *13*, 263–271, doi:10.1029/98PA00069.

Ishiwatari, R., M. Houtatsu, and H. Okada (2001), Alkenone-sea surface temperatures in the Japan Sea over the past 36 kyr: Warm temperatures at the last glacial maximum, *Org. Geochem.*, *32*, 57–67, doi:10.1016/S0146-6380(00)00151-0.

Itoh, M. (2007), Warming of intermediate water in the Sea of Okhotsk since the 1950s, *J. Oceanogr.*, *63*, 637–641.

Itoh, M., K. I. Oshima, and M. Wakatsuchi (2003), Distribution and formation of Okhotsk Sea Intermediate Water: An analysis of isopycnal climatological data, *J. Geophys. Res.*, *108*(C8), 3258, doi:10.1029/2002JC001590.

Justino, F., and W. R. Peltier (2005), The glacial North Atlantic Oscillation, *Geophys. Res. Lett.*, *32*, L21803, doi:10.1029/2005GL023822.

Lee, K.-E. (2007), Surface water changes recorded in Late Quaternary marine sediments of the Ulleung Basin, East Sea (Japan Sea), *Palaeogeogr. Palaeoclimatol. Palaeoecol.*, *247*, 18–31, doi:10.1016/j.palaeo.2006.11.019.

Liu, Z., A. C. G. Henderson, and Y. Huang (2006), Alkenone-based reconstruction of lake-Holocene surface temperature and salinity changes in Lake Qinghai, China, *Geophys. Res. Lett.*, *33*, L09707, doi:10.1029/2006GL026151.

Martin, S. R., R. Drucker, and K. Yamashita (1998), The production of ice and dense shelf water in the Okhotsk Sea polynyas, *J. Geophys. Res.*, *103*, 27,771–27,782, doi:10.1029/98JC02242.

Martinson, D. G., N. G. Pisias, J. D. Hays, J. Imbrie, T. C. Moore Jr., and N. J. Shackleton (1987), Age dating and the orbital theory of the ice ages: Development of a high-resolution 0 to 300,000-year chronostratigraphy, *Quat. Res.*, *27*, 1–29, doi:10.1016/0033-5894(87)90046-9.

Mayewski, P. A., L. D. Meeker, M. S. Twickler, S. Whitlow, Q. Yang, W. B. Lyons, and M. Prentice (1997), Major features and forcing of high-latitude Northern Hemisphere atmospheric circulation using a 110,000-year-long glaciochemical series, *J. Geophys. Res.*, *102*, 26,345–26,366, doi:10.1029/96JC03365.

Müller, P. J., G. Kirst, I. von Storch, and A. Rosell-Melé (1998), Calibration of the alkenone paleotemperature index $U^{K'}_{37}$ based on core-tops from the eastern South Atlantic and the global ocean (60°N–60°S), *Geochim. Cosmochim. Acta*, *62*, 1757–1772, doi:10.1016/S0016-7037(98)00097-0.

Nakagawa, T., H. Kitagawa, Y. Yasuda, P. E. Tarasov, K. Nishida, K. Gotanda, and Y. Sawai (2003), Asynchronous climate changes in the North Atlantic and Japan during the last termination, *Science*, *299*, 688–691, doi:10.1126/science.1078235.

Ogi, M., and Y. Tachibana (2006), Influence of the annual Arctic Oscillation on the negative correlation between Okhotsk Sea ice and Amur River discharge, *Geophys. Res. Lett.*, *33*, L08709, doi:10.1029/2006GL025838.

Ogi, M., Y. Tachibana, F. Nishio, and M. Danchenkov (2001), Does the fresh water supply from the Amur River flowing into the Sea of Okhotsk affect sea ice formation?, *J. Meteorol. Soc. Jpn.*, *79*(1), 123–129, doi:10.2151/jmsj.79.123.

Ohkushi, K., T. Itaki, and N. Nemoto (2003), Last glacial–Holocene change in intermediate-water ventilation in the northwestern Pacific, *Quat. Sci. Rev.*, *22*, 1477–1484, doi:10.1016/S0277-3791(03)00082-9.

Okazaki, Y., K. Takahashi, K. Katsuki, A. Ono, J. Hori, T. Sakamoto, M. Uchida, Y. Shibata, M. Ikehara, and K. Aoki (2005), Late Quaternary paleoceanographic changes in the southwestern Okhotsk Sea: Evidence from geochemical, radiolarian, and diatom records, *Deep Sea Res., Part II*, *52*, 2332–2350, doi:10.1016/j.dsr2.2005.07.007.

Ono, A., K. Takahashi, K. Katsuki, Y. Okazaki, and T. Sakamoto (2005), The Dansgaard–Oeschger cycles discovered in the upstream source region of the North Pacific Intermediate Water formation, *Geophys. Res. Lett.*, *32*, L11607, doi:10.1029/2004GL022260.

Prahl, F. G., and S. G. Wakeham (1987), Calibration of unsaturation patterns in long-chain keton compositions for paleotemperature assessment, *Nature*, *330*, 367–369, doi:10.1038/330367a0.

Prahl, F. G., L. A. Muehlhausen, and D. L. Zahnle (1988), Further evaluation of long-chain alkenones as indicators of paleoceanographic conditions, *Geochim. Cosmochim. Acta*, *52*, 2303–2310, doi:10.1016/0016-7037(88)90132-9.

Rabineau, M., S. Berné, J.-L. Olivet, D. Aslanian, F. Gullocheau, and P. Joseph (2006), Paleo sea levels reconsidered from direct observation of paleoshoreline position during glacial maxima (for the last 500,000 yr), *Earth Planet. Sci. Lett.*, *252*, 119–137, doi:10.1016/j.epsl.2006.09.033.

Rosell-Melé, A., et al. (2001), Precision of the current methods to measure the alkenone proxy $U^{K'}_{37}$ (and absolute alkenone abundance in sediments: Results of an interlaboratory comparison study, *Geochem. Geophys. Geosyst.*, *2*(7), doi:10.1029/2000GC000141.

Rosell-Melé, A., E. Jansen, and M. Weinelt (2002), Appraisal of a molecular approach to infer variations in surface ocean freshwater inputs into the North Atlantic during the last glacial, *Global Planet. Change*, *34*, 143–152, doi:10.1016/S0921-8181(02)00111-X.

Sakamoto, T., et al. (2006), Millennium-scale variations of sea-ice expansion in the southwestern part of Okhotsk Sea during the past 120 kyr: Age model and ice-rafted debris in IMAGES core MD01-2412, *Global Planet. Change*, *53*, 58–77, doi:10.1016/j.gloplacha.2006.01.012.

Schulz, H.-M., A. Schöner, and K.-C. Emeis (2000), Long-chain alkenone patterns in the Baltic Sea—An ocean–freshwater transition, *Geochim. Cosmochim. Acta*, *64*, 469–477, doi:10.1016/S0016-7037(99)00332-4.

Seidov, D., and B. J. Haupt (2003), Freshwater teleconnections and ocean thermohaline circulation, *Geophys. Res. Lett.*, *30*(6), 1329, doi:10.1029/2002GL016564.

Seki, O., R. Ishiwatari, and K. Matsumoto (2002), Millennial climate oscillations in NE Pacific surface waters over the 82 kyr: New evidence from alkenones, *Geophys. Res. Lett.*, *29*(23), 2144, doi:10.1029/2002GL015200.

Seki, O., K. Kawamura, M. Ikehara, T. Nakatsuka, H. Okada, and T. Oba (2004), Variation of alkenone sea surface temperature in the Sea of Okhotsk over the last 85 kyrs, *Org. Geochem.*, *35*, 347–354, doi:10.1016/j.orggeochem.2003.10.011.

Seki, O., K. Kawamura, T. Sakamoto, M. Ikehara, T. Nakatsuka, and M. Wakatsuchi (2005), Decreased surface salinity in the Sea of Okhotsk during the last glacial period estimated from alkenones, *Geophys. Res. Lett.*, *32*, L08710, doi:10.1029/2004GL022177.

Seki, O., T. Nakatsuka, K. Kawamura, S. Saito, and M. Wakatsuchi (2007), Time-series sediment trap record of alkenones from the western Sea of Okhotsk, *Mar. Chem.*, *104*, 253–265, doi:10.1016/j.marchem.2006.12.002.

Sicre, M.-A., E. Bard, U. Ezat, and F. Rostek (2002), Alkenone distributions in the North Atlantic and Nordic Sea surface waters,

Geochem. Geophys. Geosyst., *3*(2), 1013, doi:10.1029/2001GC000159.

Sikes, E. L., and M. A. Sicre (2002), Relationship of the tetra-unsaturated C_{37} alkenone to salinity and temperature: Implications for paleoproxy applications, *Geochem. Geophys. Geosyst.*, *3*(11), 1063, doi:10.1029/2002GC000345.

Stommel, H., and A. B. Arons (1960), On the abyssal circulation of the world ocean. I. Stationary planetary flow patterns on a sphere, *Deep Sea Res.*, *6*, 140–154, doi:10.1016/0146-6313(59)90065-6.

Sung, M.-K., W.-T. Kwon, H.-J. Beak, K.-O. Boo, G.-H. Lim, and J.-S. Kug (2006), A possible impact of the North Atlantic Oscillation on the east Asian summer monsoon precipitation, *Geophys. Res. Lett.*, *33*, L21713, doi:10.1029/2006GL027253.

Takizawa, T. (1982), Characteristics of the Soya Warm Current in the Okhotsk Sea, *J. Oceanogr.*, *38*, 281–292.

Talley, L. D., , and Y. Nagata (Eds.) (1995), The Okhotsk Sea and the Oyashio region, *PICES Sci. Rep. 2*, 227 pp., Inst. of Ocean Sci., Sidney, B.C., Canada.

Ternois, Y., K. Kawamura, N. Ohkouchi, and L. D. Keigwin (2000), Alkenone sea surface temperature in the Okhotsk Sea for the last 15 kyr, *Geochem. J.*, *34*, 283–293.

Thompson, D. W. J., and J. M. Wallace (1998), The Arctic Oscillation signature in the wintertime geopotential height and temperature fields, *Geophys. Res. Lett.*, *25*, 1297–1300, doi:10.1029/98GL00950.

Timmermann, A., et al. (2007), The influence of a weakening of the Atlantic meridional overturning circulation on ENSO, *J. Clim.*, *20*(19), 4899–4919, doi:10.1175/JCLI4283.1.

Volkman, J. K., A. M. Barrett, S. I. Blackburn, and E. L. Sikes (1995), Alkenones in *Gephyrocapsa oceanica*: Implications for studies of paleoclimate, *Geochim. Cosmochim. Acta*, *59*, 513–520, doi:10.1016/0016-7037(95)00325-T.

Wang, Y. J., H. Cheng, R. L. Edwards, Z. S. An, J. Y. An, J. Y. Wu, C. C. Shen, and J. A. Dorale (2001), high-resolution absolute-dated late Pleistocene monsoon record from Hulu Cave, China, *Science*, *294*, 2345–2348, doi:10.1126/science.1064618.

Yang, J. Y., and S. Honjo (1996), Modelling the near-freezing dichothermal layer in the Sea of Okhotsk and its inter-annual variations, *J. Geophys. Res.*, *101*, 16,421–16,433, doi:10.1029/96JC01091.

Zink, K.-G., D. Leythaeuser, M. Melkonian, and L. Schwark (2001), Temperature dependency of long-chain alkenone distributions in recent to fossil limnic sediments and in lake waters, *Geochim. Cosmochim. Acta*, *65*, 253–265, doi:10.1016/S0016-7037(00)00509-3.

N. Harada and M. Sato, Institute of Observational Research for Global Change, Japan Agency for Marine-Earth Science and Technology, 2-15 Natsushima-cho, Yokosuka 237-0061, Japan. (haradan@jamstec.go.jp)

T. Sakamoto, Institute for Research on Earth Evolution, Japan Agency for Marine-Earth Science and Technology, 2-15 Natsushima-cho, Yokosuka 237-0061, Japan.